S. B. MELO[1], C. C. DANTAS[2], E. A. DE O. LIMA[3], F. P. M. SIMÕES[4],
E. F. DE OLIVEIRA[2],V. A. DOS SANTOS[3]

[1]Centro de Informática,Recife, sbm@cin.ufpe.br
[2]DEN, ccd@ufpe.br, [3]UNICAP, eal@dei.unicap.br,
[4]Centro de Informática, chicofpms@hotmail.com

RECONSTRUCTION OF RADIAL CATALYST CONCENTRATION DISTRIBUTION IN AN EXPERIMENTAL TYPE FCC RISER

A gamma ray tomographic reconstruction of catalyst concentration distribution in laboratory experiments is presented. The images are generated by gamma transition measurements in an experimental riser simulating flow experiments. The manual scanner is adequate for mapping radial catalyst concentration distribution under spatial resolution of 0.002 m and density resolution of 10 kg/m^3.

Keywords: gamma tomography, catalyst concentration, experimental riser

1. INTRODUCTION

The CT - Gamma Ray Computed Tomography in process engineering actually presents a rather sophisticated technological stage. Investigations on FCC - Fluid Catalytic Cracking units and on multiphase flow in opaque reactors are increasing in continuous scientific and technological developments. Nevertheless, industrial riser tomography reveals problems that often originate from the gamma transition measurements. As it is a combination of physical measuring and mathematical reconstruction techniques, a shared approach to both should be carried out, to achieve a consistent tomography development. Following this, experimental and theoretical investigations, independent of the reactor fluid dynamics, were adopted. In addition, even most of the advanced CT processes, described in literature, use intermediate energy such as the Cs-137, 0.662 MeV, isotopic source, NaI scintillation detector, and the reconstruction technique is based on the Beer-Lambert equation. By means of this equation the transition measurement is a function of the gamma ray path length. To have a distributed density over the diameter surface it is necessary to formulate the σ density as a $\sigma = f(x, y)$ function. As the measured density is a mean value, by varying source and detector positions, $\sigma = f(x, y)$ values are the entrance to a data matrix, where x_i and y_i cross points are used to calculate local density.

Fluid dynamic models require parameters as gas and solid phase hold up, and gas and solid velocities that are based on measured variables, constant values as densities, which are taken from reference data and parameters calculated from measurement and reference data as friction coefficient and Reynolds number. The experimental data was initially modeled to evaluate instrumental precision on the measurements of: Gas flow, solid flow and the pressure drop in riser ΔP_{riser}. To estimate measured and expected values, discrete models were applied by Dantas et al., [1].

Due to variation in chemical composition and also in grain size distribution, catalyst mass attenuation coefficient data are not so easy to find and to compare. Very few papers as Azzi, et al., [2], give a mass attenuation coefficient value which is according to the described catalyst properties.

To evaluate uncertainty in density measurements, according to the Beer-Lambert equation, catalyst attenuation coefficient and gamma intensity are the main contributions to the uncertainty propagation.

2. GAMMA RAY TOMOGRAPHY

Trying to monitor the state of art of Gamma Ray Computed Tomography and foreseeing its contribution to the opaque multiphase reactors let us look at the competition. “The best known technology is CAT scanning in medicine, however process tomography instrumentation needs to be cheaper, faster and more robust.” These words were at the opening Industrial Process Tomography, held in Aizu, Japan, in September 2005. Among several fields of investigation that have taken this direction, the big effort devoted to electrical capacitance tomography - ECT and to electrical impedance tomography - EIT methods, is remarkable;

Industrial Gamma Ray Computed Tomography – CT, as the CAT scanning in medicine are photon count techniques whose intensity is a function of the attenuation coefficient. In both cases the data goes to mathematical reconstruction and computational algorithms to generate tomographic images. Along the way, gamma ray tomography has incorporated results from the fantastic development of medical tomography. At the actual stage, industrial Gamma Ray Tomography faces quite specific technological aspects, probably due to them, the search for cheaper, faster and more robust instrumentation is on the way. In a different approach from the medicine CAT, experimental set-ups in process engineering are often designed, manufactured and installed by the research groups themselves since the desired tomographic systems are still not commercially available. Some of these set -ups are rather simple and include technological innovations such as dual gamma set-ups with two ^{137}Cs gamma radiation sources (0.662 MeV) and two BGO detectors, Mudde et al., [3]. In some research institutes, the building of tomographic systems and the applied research works are developed simultaneously. Working in this direction, very sophisticated and recent instrumental development is given by the Forschungszentrum Russendorf (2005). Before 2005 they worked with a gamma tomography detector that consisted of 64 BGO scintillation crystals coupled to photomultipliers and counting electronics. The demand for higher resolution leads to the development of a high resolution tomographic gamma ray detector with 320 single detectors of 2 mm x 8mm active area based on special scintillation detectors coupled to avalanche photo diodes. The system is in an arc-like array with a Cs-137 isotopic radiation source of 5 mm diameter and 180 GBq activity. This detector performs an image resolution of approximately 3mm FWHM and a structure recovery down to 200 μm. Competitiveness inside the CT technique area includes industrial tomographic services such as the Tru-Tec Services, Inc. They offer the Cat-Scan technique that focuses on the hold-up distribution analyses and uses contour plots that might simplify the tomographic imaging process.

Such instrumental competition certainly demands detectors and coupled electronic investigations. Again as they are photon detectors, medicine leads the demand for greater resolution and real time imaging at higher energies that is pushing the scintillation array technology. An investigation on old scintillator materials like Bismute Germanate ($Bi_4Ge_3O_{12}$), producing new BGO detectors is being carried out. Position sensitive-light sensors have been driven to a great extent by medical radiography; Krus at al., [4]. From a more general trend or by specific demand the CT for engineering process is incorporating such new instrumental achievements.

In the contribution to the reactor multiphase flow study, at first, an impressive quotation should be mentioned: “It was only a decade ago that the oil industry using gamma ray techniques learned that their large diameter risers operate in the core-annular flow regime; the core is very dilute. The

core-annular structure leads to two main problems: (1) insufficient gas-solid contact, and (2) back-mixing due to non-uniform radial distributions. This unfavorable radial volume fraction distribution of solids in the riser has led to consideration of new schemes of contacting for a refinery of the 21st century", Gamwo I. and Gidaspow D. [5]. Still including radiotracer techniques as gamma ray emitter, the works from Chaouki et al., a citation in reference [6] shows that they are the most competitive techniques for investigation on large-scale multiphase flow systems. More recently Dudukovic [7] shows the advantage of combining both techniques, gamma ray computed tomography CT and computer automated radioactive particle tracking CARPT and focuses on the main contribution from CT that is phase hold- up distribution whose data are useful for validating Computational Fluid Dynamics – CDF codes. According to Dudukovic a new CT unit can achieve a spatial resolution of 2 - 3 mm but requires longer scanning times of about 4 hours and yields a density resolution better than 0.008 g/cm^3. A more sophisticated self-made tomographic set up is described by Dudukovic [7], which includes a collimated Cs-137 source positioned opposite eleven 2" sodium iodine scintillation detectors in a fan beam arrangement.

Still a recent achievement to get better resolution at low counts by means of an Alternative Minimizing Algorithm is developed by Bhusarapu et al., a citation included in reference [7].

The nuclear methods have the limitation of the Poisson nature of the photon generation process. High spatial resolution requires relative long measuring times as compared to the impedance techniques Mudde, et al., already mentioned.

Timothy et al. [8], describes a Gamma Densitometry Tomography (GDT) system that consists of a 100-mCi ^{137}Cs source and an array of 8 NaI(Tl) scintillation detectors. The source produces a fan-shaped beam that passes through the riser to the detector array, where the gamma intensity along each distinct ray is measured. The GDT and electrical impedance tomography EIT results show good agreement for both radial and axial solids-volume-fraction profiles. This means that Gamma Ray Computed Tomography is recognized as a standard method.

3. MEASURING EQUIPMENT

The measuring work of the catalyst radial density distribution in an experimental riser was carried out in a manual tomographic system. This consists of an arrangement to install a detector, a gamma source and stainless steel tubes of 0.154 m internal diameter. Such measuring equipment is used for riser irradiation scanning. The ^{137}Cs source and detector cylindrical collimators allowed a gamma beam of 0.055 m diameter to scan along the riser radius for the transition measurements. The experimental configuration given by Azzi, et al., already mentioned, was implemented in a Matlab routine. The scanning interval was defined on the gamma profile to generate the density data matrix. The Compton scattering contribution was minimized by collimator length and additionally a computer program was written to improve spectrum evaluation under heavy Compton interference; Costa, et al., [9].

Discrete models for modeling riser profile, space resolution and density resolution were implemented by computer programs. Static and simulated flow experiments were carried out to test catalyst concentration reconstruction. Density radial distributions were analyzed in 3D graphics, according to metrological criteria for data visualization, prior to the image reconstruction.

4.MATHEMATICAL RECONSTRUCTION

The objective here is to reconstruct the graph of the density function from the gamma ray trajectories mean density values. The experimental configuration used in this work assumes the trajectories are parallel to the edges of an equilateral triangle in which the riser is inscribed. Since in each of the three directions the amount of trajectories is the same, and they are uniformly spaced, this configuration induces a triangulation in this large triangle, formed only by mini congruent equilateral triangles. This arrangement favors accuracy, since any vertex in a mini-triangle lies in three trajectories, which means that the corresponding function value is present in three equations. Other three-direction-configurations will lead to irregular triangles, with a larger number of vertices, generally present in two trajectories each. Sparser areas will present larger errors than denser ones.

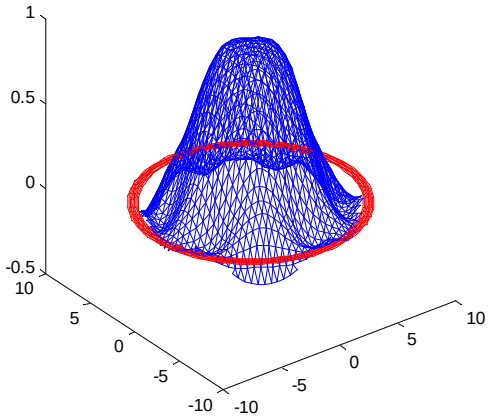

Fig. 1. Reconstruction of the core experiment with the Bezier method.

The novelty of this work is to present and test with experimental data a reconstruction more suitable to this scenario of equilateral triangulation: the non-parametric Bézier triangles, to be defined in the next section. The argument for this kind of functions is a triplet of *barycentric coordinates*. If it is given three non-collinear points in the plane, it is possible to write any other point in the plane as a barycentric combination of these three points. Let **a**, **b** and **c** be three non-collinear points in the plane. Then we may say that $\mathbf{p} = u\mathbf{a} + v\mathbf{b} + w\mathbf{c}$, where $u + v + w = 1$, and **p** is an arbitrary point in the plane. We say that (u, v, w) is a triplet of barycentric coordinates of **p** with respect to **a**, **b** and **c**. If **p** is in the interior of the triangle determined by **a**, **b** and **c**, then u, v and w take values in the interval [0, 1]. The points where $u = k$, where k is a real constant, form a straight line parallel to the line segment between **b** and **c**. The points where $v = k$, where k is a real constant, form a straight line parallel to the line segment between **a** and **c**. It is analogous for $w = k$, and the segment between **a** and **b**. For instance, $w = 1$, 1/3 and 0 correspond respectively to the lines passing through point **c**, the triangle's barycenter and both points **a** and **b**.

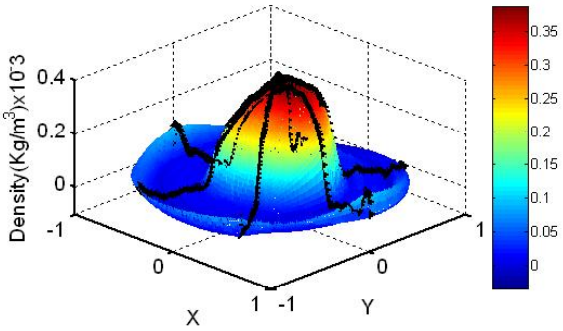

Fig. 2. Sinogram of the three experimental projections from core experiment.

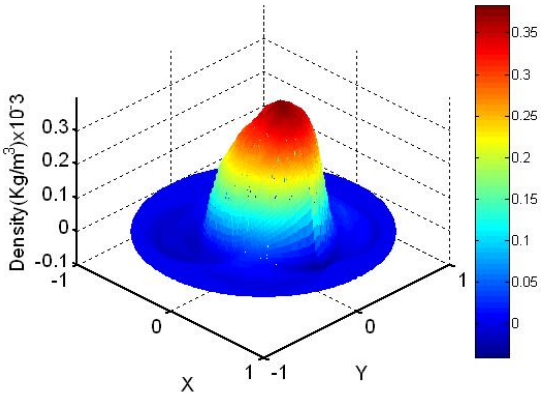

Fig. 3. Sinogram reconstruction by FBP with 180 projections.

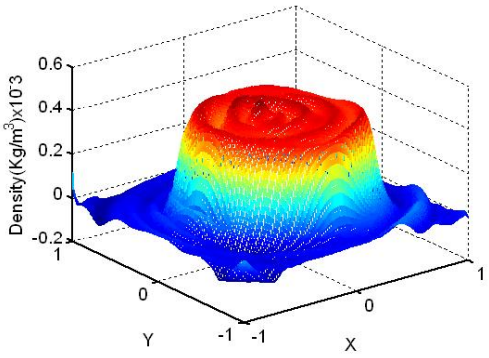

Fig. 4. Reconstruction by FBP from the three experimental projections and interpolation.

4.1 Bézier Triangles

The non-parametric Bézier triangle is a patch of a polynomial surface, in which each variable takes barycentric coordinates with respect to a given triangle in the domain. These barycentric coordinates are arguments for the Bernstein Basis, which become weights for the weighted average of the density values associated with the intersections of the gamma rays. More precisely, using the notation of [10]:

$$D(\mathbf{u}) = \sum_{|\mathbf{i}|=n} B_{\mathbf{i}}^{n}(\mathbf{u}) b_{\mathbf{i}}\,. \qquad (1)$$

$D(\mathbf{u})$ is the proposed density function, where $\mathbf{u} = (u, v, w)$, with $u + v + w = 1$ the barycentric coordinates of the point for which the density value is required, $\mathbf{i}$ is a triple-index-value ijk, used to identify each intersection point and its density value, $b_{\mathbf{i}}$. In the formula, $|\mathbf{i}| = n$ means that $i + j + k = n$. The summation runs over all possible positive integer values of ijk subject to this condition.
The Bernstein polynomials are defined as:

$$B_{\mathbf{i}}^{n}(\mathbf{u}) = \binom{n}{\mathbf{i}} u^{i} v^{j} w^{k},$$

where

$$\binom{n}{\mathbf{i}} = \frac{n!}{i!\,j!k!}.$$

The density values $b_{\mathbf{i}}$ are called control densities, and are associated with the control points of the non-parametric triangular Bézier patch:

$$\left(\frac{i}{n} \quad \frac{j}{n} \quad \frac{k}{n} \quad b_{\mathbf{i}} \right)^{t},$$

for each i, j, k so that $i + j + k = n$. The graph of D interpolates $b_{\mathbf{i}}$, where $\mathbf{i} = ijk$, where $i = n$, $j = n$ or $k = n$, the three ends of the triangle. The Bernstein polynomials form a basis for the space of all polynomials in two variables (since $u + v + w = 1$). Therefore, any polynomial surface is a Bézier surface. Another important property is that they satisfy the *unit partition* condition:

$$\sum_{|\mathbf{i}|=n} B_{\mathbf{i}}^{n}(\mathbf{u}) \equiv 1 \qquad (2)$$

independently of $\mathbf{u} = (u, v, w)$, with $u + v + w = 1$. Since u, v, w in this present work's application are non-negative, it will always be obtained as a convex combination of the control density values when computing an arbitrary point's density value. That is a desirable quality, as far as the error analysis is concerned. In the next section it is shown how the control densities are found.

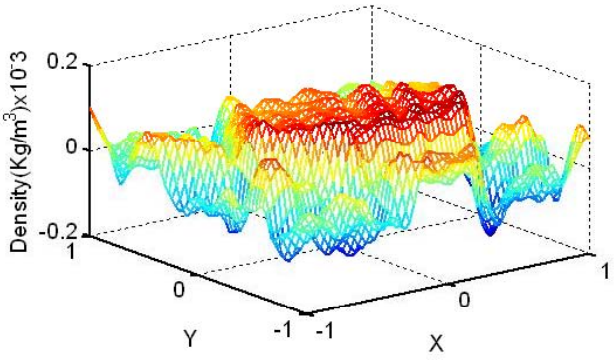

Fig. 5. Core reconstruction by FBP with the three experimental projections.

4.2 Least Squares Approach

Here it is proposed to estimate the control densities through an application of the least squares method to the function defined in the Eq. (1). We suggest that the average of the control densities along a gamma ray trajectory is a good estimate for the actual density value from the experiments. It is not difficult to realize that the bigger the number of trajectories, the better the estimation. In barycentric coordinates, the points in a given gamma ray trajectory can be characterized as those in which one of the coordinates is a fixed positive number, less than or equal to 1. According to our choices for the triangle configuration, one such number is always of the type $i/(m - 1)$ for some i in $\{0, 1, ..., m - 1\}$, where m is the number of trajectories in each edge of the triangle that circumscribes a riser's section. We may establish that $\delta_{u,i}$, $\delta_{v,j}$ and $\delta_{w,k}$ are the acquired experimental density values associated with the trajectories in which $u = i/(m - 1)$, $v = j/(m - 1)$ and $w = k/(m - 1)$, respectively. Let $\mathbf{i}/m$ be the triplet $(i/(m - 1), j/(m - 1), k/(m - 1))$. In the trajectory where $u = i_0/(m - 1)$ for some i_0, we may say that the average density of the approximating function from (1) ideally should be equal to the corresponding acquired experimental density:

$$\frac{1}{m - i_0} \sum_{\substack{|\mathbf{i}|=m-1 \\ i=i_0}} D(\mathbf{i}/m) = \delta_{u,i_0} .$$

Substituting (1) in this equation we get:

$$\frac{1}{m - i_0} \sum_{\substack{|\mathbf{i}|=m-1 \\ i=i_0}} \sum_{|\mathbf{j}|=n} b_{\mathbf{j}} B_{\mathbf{j}}^n(\mathbf{i}/m) = \delta_{u,i_0} ,$$

after rearranging it:

$$\sum_{|\mathbf{j}|=n} b_{\mathbf{j}} \left(\frac{1}{m - i_0} \sum_{\substack{|\mathbf{i}|=m-1 \\ i=i_0}} B_{\mathbf{j}}^n(\mathbf{i}/m) \right) = \delta_{u,i_0} ,$$

similarly, for the trajectories where $v = j_0/(m - 1)$ for some j_0 in $\{0, 1, ..., m - 1\}$ and $w = k_0/(m - 1)$ for some k_0 in $\{0, 1, ..., m - 1\}$, we obtain:

$$\sum_{|\mathbf{j}|=n} b_{\mathbf{j}} \left(\frac{1}{m - j_0} \sum_{\substack{|\mathbf{i}|=m-1 \\ j=j_0}} B_{\mathbf{j}}^n(\mathbf{i}/m) \right) = \delta_{v,j_0}$$

and

$$\sum_{|\mathbf{j}|=n} b_{\mathbf{j}} \left(\frac{1}{m - k_0} \sum_{\substack{|\mathbf{i}|=m-1 \\ k=k_0}} B_{\mathbf{j}}^n(\mathbf{i}/m) \right) = \delta_{w,k_0} .$$

These are the $3m$ rows of the overdetermined system $AX = b$, where X contains the unknowns $b_{\mathbf{i}}$. The least squares problem is set by the normal equations: $A^T AX = A^T b$.

The symmetric coefficient matrix of this linear system of equations possesses $(n + 1)(n + 2)/2$ rows and columns. Typically, when $n \leq \frac{\sqrt{24m+1}-3}{2}$, the least squares problem will return a unique solution.

Due to Eq. (2) and the fact that the Bernstein polynomials are non-negative, provided that the arguments are also non-negative, the error propagation is minimized when compared to other bases, such as the monomial or Lagrangean ones. Another advantage of this approach is the coordinate system: the gamma ray trajectories are specified by a constant ($w = k$, for instance) calling for less arithmetic operations than the affine equation $y = ax + b$. The homogeneity of the mini-triangles makes it easier to specify the intersections between the trajectories ($u = i/(m - 1)$, $v = j/(m - 1)$ and $w = k/(m - 1)$) benefiting in its turn each estimated trajectory mean density value. Yet another important characteristic is its symmetry in the domain. There is no privileged orientation, and the error is expected to be homogeneously distributed along the triangle area.

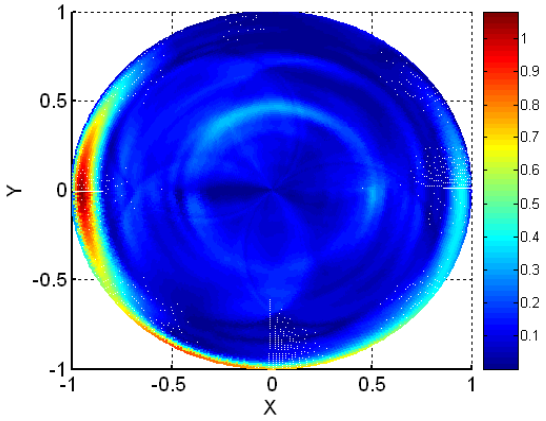

Fig. 6. Error distribution by comparing experimental and reconstructed sinograms.

In order to evaluate the use of Bézier triangles for the tomographic reconstruction, we have investigated its errors in a simulated experiment, and performed a comparison against the Filtered Back-Projection method. About this, it is necessary clarify a few points on the experimental setup used in a first- generation tomographer. The number of projections which is variable under a practical point of view is generally not greater than 10. The time involved in the process of data acquisition is crucial for the experiment to be significant. Our proposed method is more suitable for this type of scenario, and it is organized much like in the work of M. Azzi et al. As shown in Fig. 3, if there were no such restrictions, the Filter Back Projection – FBP, would provide a near perfect reconstruction, with 180 projections. On the other hand, if only 3 projections are used, the FBP results are not satisfactory. Nevertheless, FBP with only 3 projections may be improved substantially if 180 projections are obtained from these three experimental projections through linear interpolation. This is adequate for radial symmetrical graphs. The alluded interpolation occurs right before the projections are Fast-Fourier-Transformed, which is part of the inverse Radon transform.

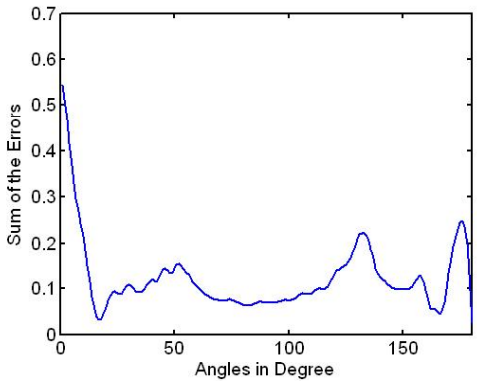

Fig. 7. A sum of errors estimation from each trajectory.

5. RESULTS

The results presented are from static simulation of a core flow. The catalyst density will be given as

$$\rho_{core}(x,y) = \begin{cases} 1 \text{ if } x^2 + y^2 \leq s \\ 0 \text{ if } x^2 + y^2 \geq s \end{cases},$$

where 0 and 1 are the interval of a given density and m = (c - y), with c and y as chordal lengths for circle s and for the riser.

To implement the reconstruction technique, a computational algorithm by means of which catalyst concentrations in static experiments are presented, was written. The core experiments are shown in Figs. 1 to 4.

In the annular experiment an error of 13 % at the centre and of 5 % for the extremities was fond. In cores a 10 % error on the extremities and of 1% at the centre was evaluated.

6. CONCLUSIONS

To improve the least square approximation it is suggested to take the integral of density function along each trajectory, divided by the length of the trajectory inside the riser, instead of simply averaging the function values at the intersections between the trajectory with other trajectories. Another improvement may be to devise a method to estimate the function values in the trajectories, and then to use an interpolation method, such as a C^1 piecewise cubic Bézier triangles Kong, [11]. Considering also functions that are implemented in the Matlab software as the FBP method. Interpolation can improve significantly the image reconstruction from a reduced number of projections, like in the three experimental projections given in Figure 4. Such a method seems to be promising for catalyst density reconstruction by optimizing the projections number/minimizing errors in further experiments. Error estimation is still usual in all the scientific and technological investigations and uncertainty evaluation probably will be more required for the future of industrial tomography. A few examples might support such prediction: better knowledge about the process

data and determination of tomographic parameters is required. There is a trade-off between speed of response, spatial resolution and resolution of the imaged parameter, [12].

ACKNOWLEDGMENTS

The CTPETRO\FINEP\PETROBRAS supported the work, the authors wish to thank Dr. Waldir Martignoni, SIX and Eng. Claudia de Lacerda Alvarenga, CENPES/PETROBRAS, for their suggestions and assistance.

REFERENCES

1. Dantas C. C., dos Santos V. A., de O. Lima E. A., Melo, S. B.: *Advanced Mathematical & Computational Tools In Metrology VII*, (2006), pp. 284-288; Series on Advanced in Mathematics for Applied Sciences - vol. 72; World Scientific Publishing Co. Pte. Ltd.
2. Azzi M., Turlier P., Bernard J. R., Garnero L.: *Mapping solid concentration in a circulating fluid bed using gammametry*, Powder Technology, vol. 67, pp. 27-36, 1991.
3. Mudde R. F., Bruneau P. R. P., Van de Hagen T. H. J. J.: Ind., Eng., Chem., Res., 44, 6181-6187, 2005.
4. Krus D. J., Novak W. P., Perna L.: *Hard X – Ray, Gamma Ray and Neutron Detector Physics*. SPIE International Symposium on Optical Science, Engineering and Instrumentation. SPIE vol. 3768, 1999.
5. Gamwo I., Gidaspow D.: UCR Annual Report, 1999.
6. Dudukovic M. P.: *Opaque Multiphase Reactors: Experimentation, Modeling and Troubleshooting*, Oil & Gas Science and Technology – Rev. IFP. vol. 55, no. 2. pp. 135-158, 2002.
7. Dudukovic M. P.: Proc. Symposium dedicated to Prof. Akira Hirata, Japan, 2005.
8. O'Hern T., Trujillo S. M., Torczynski J. R., Tortora P. R., Ceccio S. L.: *AIChi Technical Program in Images*, November 2005.
9. da Costa P. C. L., Dantas C. C., Lira C. A. B. O., dos Santos V.A.: *A Compton filter to improve photopeak intensity evaluation in gamma ray spectra,* Nucl. Inst. and Meth. B 226, pp. 419-425, 2004.
10. Farin G.: *Curves and Surfaces for CAGD*: a Practical Guide. 4th edition, Academic Press 1996.
11. Kong V. P., Ong B. H., Saw K. H.: *Range Restricted Interpolation Using Cubic Bézier Triangles*. WSCG'2004, Feb. 2-6, 2004, Plzen- Czech Republic.
12. Johansen J.A.: *Nuclear tomography methods in industry,* Nuclear Physics, A 752, pp. 696c-705c, 2005.